

Received April 8, 2019, accepted May 4, 2019, date of publication May 7, 2019, date of current version May 17, 2019.

Digital Object Identifier 10.1109/ACCESS.2019.2915280

Detailed Modeling and Experimental Assessments of Automotive Dry Clutch Engagement

ZHENGFENG YAN¹, FUWU YAN², JIEJUNYI LIANG^{1,2}, AND YALIN DUAN¹

¹School of Automotive and Transportation Engineering, Hefei University of Technology, Hefei 230009, China

²School of Automotive Engineering, Wuhan University of Technology, Wuhan 430070, China

Corresponding author: Jiejunyi Liang (jiejunyi.liang@gmail.com)

This work was supported in part by the State Scholarship Fund of China Scholarship Council under Grant 201706695018.

ABSTRACT The characteristics of the clutch engagement process would have significant influences on the torque transmissibility and operation comfort. However, some crucial components are simplified in many previous literature, which would cause imprecision. Therefore, it is important to build a detailed mathematical model of these components and inspect the whole process of clutch engagement. In order to improve the torque transmissibility and achieve better pedal releasing comfort, solutions based on the modeling of the clutch cover assembly and the friction disc assembly, the analysis of the clamping force and the releasing characteristics of the release bearing are proposed in this paper. Furthermore, models of the crucial components such as the diaphragm spring, which connects the straps and cushion plate, are built and the corresponding mechanical properties are analyzed. Based on the manufacturing tolerance, the life cycle, and the wear properties, diaphragm spring correction formula is proposed by referring to Almen-Laszlo method. On the system level, the whole engagement process is divided into four stages because of the differences between the engaging and disengaging processes, which would affect the pedal releasing comfort in the manual transmission system and the shifting quality in the automated transmission system. To demonstrate the effectiveness of the proposed method, detailed mathematic models are built and the corresponding experiments are conducted.

INDEX TERMS Mathematical modeling, clutch engagement, cushion characteristics, torque transmissibility, operation comfort.

I. INTRODUCTION

Automotive dry clutch which has been widely adopted in manual transmission system [1] and automated manual transmission (AMT) system [2] as the key launching and shifting component and has attracted the attention of many researchers both from the academic and the industry [3]. Various successful products such as the diaphragm spring clutch, self-adjusting clutch, travel adjusted clutch and pre-damped clutch damper catering to different needs have been developed by Valeo, LUK, SACHS and other companies which boost the development of clutch technology [4]. Although the development of new energy vehicles [5], [6] and automatic transmission technology [7] inspires more advanced structure and complex system, the dry clutch is still widely used because of its efficiency, robustness and low

manufacturing cost [8]–[10]. As the engagement [11] and disengagement [12] processes have significant influence on the shifting smoothness and driving comfort and directly affect the torque transmission ability, in the meantime, the development of intelligent control approaches require higher precision [13], [14], more accurate clutch models are imperative to inspect and improve the vehicle longitudinal dynamics and torque transmissibility, which could both improve the manipulating comfort in manual transmission system and help develop more advanced control strategy in automated transmission systems such as AMT and dual clutch transmission (DCT) [15], [16].

For system level transmission modeling, methods such as graph theory model, screw theory and bond graph model are widely adopted to establish the vehicle transmission system dynamics equations by combining the vehicle power system with the transmission system [17]. In [18], [19], bond graph modeling is used to reveal the power flow of the transmission

The associate editor coordinating the review of this manuscript and approving it for publication was Xu Chen.

system and the torque and speed relationships between different components. Paul D. Walker *et al.* focused on the different degrees of freedom of a DCT system in [20] establishing a dynamic model and the corresponding torque calculation formulations. In [21], [22], the clutch dynamic model is included, and the corresponding equations are built. As to the component level, the clutch cover assembly and the friction disc assembly should both be considered to achieve a high level of accuracy. In [23], the clutch cover assembly load characteristics and the disc assembly axial cushion characteristics are analyzed, and the torque calculation formulation is defined according to the pressure-based equivalent radius. Based on the frictional characteristics of clutch engagement and disengagement, the static friction coefficient and dynamic friction coefficient are used respectively to set up the torque transfer equations of the corresponding phase [24].

In order to achieve the function of transmitting torque and cutting off the power during the process of launching and shifting [25], four positions should be defined as engaged position, disengaging position, disengaged position and engaging position. Due to the similarity of the disengaging and engaging process, many literatures regard them as the same process where the working state of the clutch is divided into three types: the sliding process, engaged and disengaged state, and ignore the influence of its differences [13]. Although the engaging and disengaging processes in the clutch could be treated as sliding process, the loading and releasing forces would be affected by the hysteresis characteristics of the elastic elements, manufacturing and assembly tolerances. Clutch disengagement characteristics mainly affects the vehicle manipulating comfort [26] in manual transmission systems and could be used in developing advanced control strategy in automated systems [27]. The evaluation and the corresponding experiments of the ergonomics and biomechanical method such as how to operate a clutch pedal and how to measure the associated comfort have been conducted in [28], [29]. Although the engagement and disengagement characteristics have been included in the aforesaid literature, they are treated as isolated problems, without being considered systematically. The torque transmissibility and operating comfort should be investigated in the design process at the same time. The factors, including the clamping force of the clutch cover assembly, the releasing characteristics of the release bearing, the characteristics of the friction disc assembly cushion, the clutch release system and the engaging speed would affect the engagement and disengagement performance of the clutch. As a result, by considering the disengaging and engaging process as different processes, the modeling and analysis of these four stages will be conducted systematically and measured using different criteria.

Constructing a system level dynamic model [30] with corresponding clutch cover assembly and friction disc assembly and investigating the four stages separately cannot guarantee the accuracy of the system because of the nonlinearity, delay, interference parameters and mutual influence among the clutch driving part (cover assembly), the secondary part

(disc assembly) and the operating mechanism which come from the constituent components such as the diaphragm spring, the strap, the cushion plate and the friction facing materials. In [13], [23], the mutual activities of the cover assembly and disc assembly during the engagement of clutch have been considered as well as the influence of the key parts such as the diaphragm spring and the cushion plate. Relevant experiments verified the effectiveness and accuracy of the established dynamic mathematical model. Although these studies considered the influences of the characteristics of several components, the accuracy is still compromised by neglecting the differences between the clutch cover assembly load characteristics and the mechanical properties of the diaphragm spring [31]. Moreover, the influence of the strap on the load characteristics of the cover assembly should also be considered according to the different structures of the clutch [32], especially the no hook clip clutch structure (e.g., VALEO company CP structure). As a result, it is necessary to establish the detailed model by reorganizing and including the detail structures and dynamic equations of the diaphragm spring, the strap and the cushion plate systematically. Then the optimized design would meet the requirements of vehicle transmission system.

The main focus of this paper can be summarized as: 1) The dynamic responses of diaphragm spring such as the hysteresis characteristics and the influence of manufacturing tolerance are investigated. 2) The cushion plate transferred force is considered to simulate the cover assembly releasing force. 3) The influence of the detailed modeling on the clutch pedal characteristics.

In this paper, the modeling, control and experiments are conducted on a push-type diaphragm spring clutch for passenger vehicles and the following works are proposed. On system level, the four stages of the clutch are defined and the corresponding dynamic models with the mechanical properties are established and analyzed in the Section 2, as well as the establishment of the system solutions for the dry clutch torque transmissibility and pedal releasing comfort based on the analysis of the clutch cover assembly load and the releasing characteristics of the release bearing, the friction disc cushion characteristics and the clutch release system. For specific constituent components, models and the corresponding mechanical properties of key parts in the clutch such as the diaphragm spring, the strap and the cushion plate will be investigated in Section 3. In Section 4, relevant experiments and analyses will be carried out to demonstrate the effectiveness of the proposed method.

II. SYSTEM MODELING AND CONTROL

In order to investigate the torque transmissibility of the clutch and achieve accurate clutch release control, a system level dynamic model is necessary. Four different working stages need to be defined along with the corresponding dynamic equations. Both detailed mathematical models of the clutch cover assembly and the disc assembly should be constructed to reveal the characteristics of the transmitted torque.

To achieve better engaging and releasing control, the characteristics and influence of the clamping forces and the releasing forces will also be investigated and tested.

A. CLUTCH WORKING POSITIONS

According to the operation process of the clutch, the working states are divided into four positions: completely engaged position, disengaging position, completely disengaged position and engaging position. The detailed descriptions of each state are given as follows and the lumped models are shown in Figure 1.

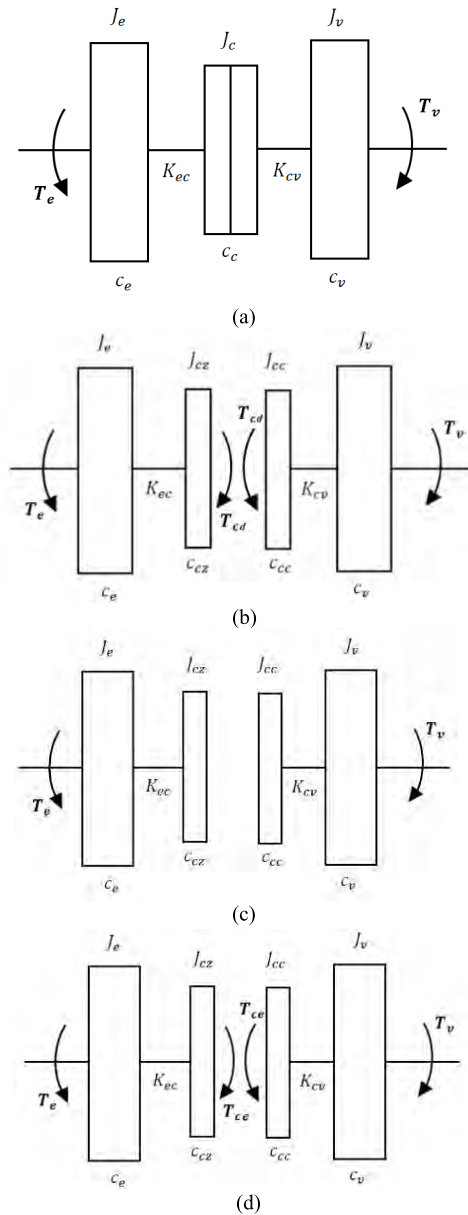


FIGURE 1. The transmission system dynamic models for different stages.

1) ENGAGED POSITION

The diaphragm spring pushes the pressure plate, clamping the clutch disc assembly to the flywheel and transmitting the torque from the engine to the output shaft. In this stage,

the clutch cover assembly and disc assembly are combined to rotate at the same speed.

As shown in Figure 1 (a), the system can be regarded as a three-degree of freedom system, and the dynamics equation can be expressed as [19]:

$$\begin{cases} J_e \ddot{\theta}_e + C_e \dot{\theta}_e + K_{ec} (\theta_e - \theta_c) = T_e \\ J_c \ddot{\theta}_c + C_c \dot{\theta}_c + K_{ec} (\theta_c - \theta_e) + K_{cv} (\theta_c - \theta_v) = 0 \\ J_v \ddot{\theta}_v + C_v \dot{\theta}_v + K_{cv} (\theta_v - \theta_c) = -T_v \end{cases} \quad (1)$$

where T_e and T_v are the engine output torque and the equivalent resistance moment of the vehicle. J_e , J_c and J_v are the equivalent moment of inertia of the crankshaft and connecting rod mechanism, the clutch, and the equivalent moment of inertia of the propeller shaft and all vehicle after the output shaft of the clutch. C_e , C_c and C_v are damping coefficients of the engine, the clutch and the vehicle. K_{ec} and K_{cv} are the torsional stiffness of the connecting shaft between the engine and the flywheel, and the torsional stiffness between the clutch disc assembly and the output shaft of the clutch, respectively. θ with footnotes represent the corresponding angular displacements

2) DISENGAGING POSITION

The clutch disengaging is a continuous process where the releasing bearing pushes the center of the diaphragm spring to the flywheel, then the clutch disc assembly would gradually move away from the flywheel, leading to sliding friction between the flywheel and the disc assembly.

The dynamic model of the drivetrain in the clutch disengaging process is shown in Figure 1 (b). Dry friction exists between the clutch cover assembly and disc assembly in the sliding condition and the sliding torque is represented by T_{cd} . The system dynamic equations are:

$$\begin{cases} J_e \ddot{\theta}_e + C_e \dot{\theta}_e + K_{ec} (\theta_e - \theta_{cz}) = T_e \\ J_{cz} \ddot{\theta}_{cz} + C_{cz} \dot{\theta}_{cz} + K_{ec} (\theta_{cz} - \theta_e) = -T_{cd} \\ J_{cc} \ddot{\theta}_{cc} + C_{cc} \dot{\theta}_{cc} + K_{cv} (\theta_{cc} - \theta_v) = T_{cd} \\ J_v \ddot{\theta}_v + C_v \dot{\theta}_v + K_{cv} (\theta_v - \theta_{cc}) = -T_v \end{cases} \quad (2)$$

where J_{cz} and J_{cc} are the equivalent moment of inertia of the flywheel and clutch cover assembly, and the clutch disc assembly. C_{cz} and C_{cc} are damping coefficients of the clutch cover assembly and the clutch disc assembly.

3) DISENGAGED POSITION

The release bearing is pushed to the specified position where the clutch disc assembly is completely disengaged with pressure plate and the flywheel. The axial clamping force becomes zero and the transmitted torque is also zero.

As shown in Figure 1 (c), the disc assembly is disconnected from the cover assembly and flywheel, the torque from the engine to the clutch disc assembly is zero. The corresponding

kinetic equation is as follows:

$$\begin{cases} J_{ee}\ddot{\theta}_e + C_e\dot{\theta}_e + K_{ec}(\theta_e - \theta_{cz}) = T_e \\ J_{cz}\ddot{\theta}_{cz} + C_{cz}\dot{\theta}_{cz} + K_{ec}(\theta_{cz} - \theta_e) = 0 \\ J_{cc}\ddot{\theta}_{cc} + C_{cc}\dot{\theta}_{cc} + K_{cv}(\theta_{cc} - \theta_v) = 0 \\ J_v\ddot{\theta}_v + C_v\dot{\theta}_v + K_{cv}(\theta_v - \theta_{cc}) = -T_v \end{cases} \quad (3)$$

4) ENGAGING POSITION

The releasing force gradually reduces as well as the displacement of the releasing bearing resulting in the increase of the pressure plate clamping force. In this stage, relative sliding happens between the cover assembly and the disc assembly. Figure 1 (d) shows a similar process as in the disengaging process but with a different torque T_{ce} since the loading and releasing forces would be affected by the hysteresis characteristics of the elastic elements, manufacturing and assembly tolerances, the transmitted torques are different due to the different clamping forces. The differences between them will be shown in the following sections.

$$\begin{cases} J_e\ddot{\theta}_e + C_e\dot{\theta}_e + K_{ec}(\theta_e - \theta_{cz}) = T_e \\ J_{cz}\ddot{\theta}_{cz} + C_{cz}\dot{\theta}_{cz} + K_{ec}(\theta_{cz} - \theta_e) = -T_{ce} \\ J_{cc}\ddot{\theta}_{cc} + C_{cc}\dot{\theta}_{cc} + K_{cv}(\theta_{cc} - \theta_v) = T_{ce} \\ J_v\ddot{\theta}_v + C_v\dot{\theta}_v + K_{cv}(\theta_v - \theta_{cc}) = -T_v \end{cases} \quad (4)$$

B. CLUTCH TORQUE TRANSMISSIBILITY

After constructing the system level dynamic equations, the detailed clutch model should be investigated which would have a significant influence on the torque transmissibility and the control system. As the torque and speed responses during launching and shifting are two main features of a clutch system, these characteristics would be adopted to measure the performance of the proposed model in this paper. Figure 2 shows the detailed structure of the investigated dry clutch which is composed of a cover assembly, a disc assembly and a clutch operation system.

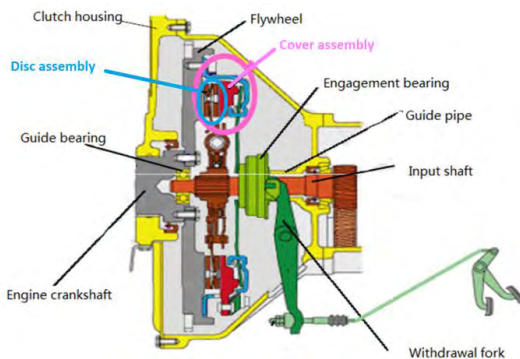


FIGURE 2. Structure of the clutch and the operation system.

Figure 2 shows the detailed structure of the investigated single-disc dry clutch which is composed of a cover assembly, a disc assembly and a clutch operation system. While the torque model, diaphragm spring modeling, strap modeling,

cushion plate modeling, which are detailed in Section II.B and Section III.

The flywheel is fixed on the crankshaft and the cover assembly (clutch cover, diaphragm spring and the pressure plate) is bolted to the flywheel, thus they rotate at the engine speed. The clutch torque is generated by the friction of the frictional pads. The clutch disc is fixed at the gearbox input shaft to transmits the generated torque to the driveline [33]. In addition, there is a torsional damper in the clutch disc to damp the oscillations of engine torque [34].

During disengagement, the release bearing connected to the release fork is pushed against the diaphragm spring under an axial force. Since the diaphragm spring act as a lever, the force direction is reversed by the diaphragm spring and the pressure plate is relieved. With the help of leaf springs, the clutch is disengaged (open) and no frictional torque is transmitted by the clutch. When the cushion spring is completely compressed by the pressure plate the clutch is closed, whereas when the cushion spring is not compressed the clutch is open [21].

There are two different methods about the clutch torque calculation model owing to the different assumptions. One is the uniform pressure method, which assumes the uniform distribution of the pressure on the friction surface. The other is the uniform wear method, which assumes uniform distribution of wear on the friction surface.

In order to be safe, reliable and convenient to calculate, the uniform pressure method is adopted here to calculate clutch torque. With the development of the product structure of clutch, integrated cushion plate structure which is shown in Figure 3 is prevailing among passenger cars.

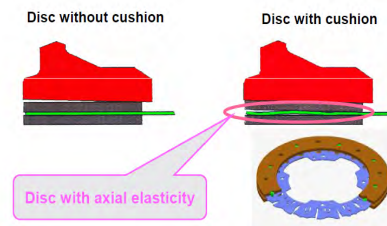


FIGURE 3. Disc assembly cushion plate schematic diagram.

The clamping force [23] between flywheel and pressure plate can be written as

$$F_{pp} = \int_0^{2\pi} \int_{R_1}^{R_2} \sigma(\rho, \varphi, F_{pp}) \rho d\rho d\varphi \quad (5)$$

where F_{pp} is for the clamping force of the pressure plate and F_{rb} represents the releasing force of clutch. ρ and φ are the radial and angular variables of the friction face, the R_1 and R_2 are the inner and outer radii of the clutch friction face and σ is the pressure distribution on the friction face.

The sliding torque of clutch T_c can be written as

$$T_c = z \int_0^{2\pi} \int_{R_1}^{R_2} \tau(\rho, \varphi, F_{pp}) \rho^2 d\rho d\varphi \quad (6)$$

where τ is the distribution of tangential stress along the friction surfaces of the clutch, z is the friction facing number.

Coefficient R_μ can be introduced and defined as

$$R_\mu = \frac{\int_0^{2\pi} \int_{R_1}^{R_2} \tau(\rho, \varphi, F_{pp}) \rho^2 d\rho d\varphi}{\int_0^{2\pi} \int_{R_1}^{R_2} \sigma(\rho, \varphi, F_{pp}) \rho d\rho d\varphi} \quad (7)$$

In order to obtain an expression for R_μ , a typical assumption made in friction mechanics is [35]

$$\tau(\rho, F_{pp}) = \mu(\rho\omega_{fc}) \sigma(\rho, F_{pp}) \quad (8)$$

where $\mu(v)$ is the dynamic friction coefficient, with v being the tangential velocity. Since $v = \rho\omega_{fc}$, $\omega_{fc} = \omega_f - \omega_c$, where ω_f is the angular velocity of the disc assembly and ω_c is the angular velocity of the cover assembly. The following expression can be generated

$$\mu(\rho\omega_{fc}) = \text{sign}(\rho\omega_{fc}) \mu \quad (9)$$

If σ is assumed to be constant, then (7) and (8) become

$$R_\mu = \text{sign}(v) \cdot \mu \frac{2R_2^3 - R_1^3}{3R_2^2 - R_1^2} \quad (10)$$

where μ is the friction coefficient.

The simplified expression of the relationship between the friction torque of the clutch T_c and the clamping force F_{pp} is

$$T_c = z\mu \frac{2R_2^3 - R_1^3}{3R_2^2 - R_1^2} F_{pp} \quad (11)$$

According to the analysis of the four stages of the clutch operation, the equations of transmitted torque in the four states can be determined as follows [20]

$$T_c = \begin{cases} T_{avg}, & \text{Engaged position} \\ z\mu_D \frac{2R_2^3 - R_1^3}{3R_2^2 - R_1^2} F_{ppd}, & \text{Disengaging position} \\ 0, & \text{Disengaged position} \\ z\mu_D \frac{2R_2^3 - R_1^3}{3R_2^2 - R_1^2} F_{ppe}, & \text{Engaging position} \end{cases} \quad (12)$$

where T_{avg} is output average torque of engine for engaged state, F_{ppd} is the clamping force between pressure plate and flywheel under disengaging process, μ_D is the dynamic coefficient of friction facing and F_{ppe} is the clamping force between pressure plate and flywheel under disengaging process.

At engaged position, the clutch torque capacity is T_{cc} .

$$T_{cc} = z\mu_s \frac{2R_2^3 - R_1^3}{3R_2^2 - R_1^2} F_{pp} \quad (13)$$

where μ_s is the static friction coefficient of friction face.

C. CLUTCH DISENGAGING PROCESS AND CLUTCH CLAMPING AND RELEASING FORCE ANALYSIS

The most significant difference of clutch engaging process and disengaging process could be revealed in the pedal releasing process in manual transmission system and the clutch releasing control in automated transmission system. The different characteristics of the clamping force in these two processes would affect the vehicle longitudinal dynamic performance and the driving comfort. To investigate the influence of the disengaging process, the structure of the hydraulic releasing system should be demonstrated first, and it is shown in Figure 4.

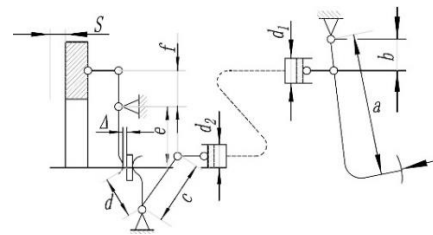


FIGURE 4. The diagram of the hydraulic clutch manipulating mechanism.

The pedal travel S consists of the free travel S_1 and the work load travel S_2 [36].

$$S = S_1 + S_2 = \left(S_{0f} + z\Delta S \frac{e}{f} \right) \frac{acd_2^2}{bdd_1^2} \quad (14)$$

where S_{0f} is the free travel of the releasing bearing, transferring to the free travel S_1 on the pedal. d_1 and d_2 are the diameter of the master cylinder and the slave cylinder, respectively. ΔS is the gap between the friction element surfaces when the clutch is disengaged; a, b, c, d, e and f are the lever dimensions. The pedal force F_f could be calculated using the following equation:

$$F_f = \frac{F_{rb}}{i_\Sigma \eta} + F_s \quad (15)$$

where i_Σ is the total transmission ratio of the operating mechanism and $i_\Sigma = \frac{aced_2^2}{bdf d_1^2}$. η is the mechanical efficiency and F_s is the required pedal force to overcome the pull of the return spring.

Normally, the characteristics of the diaphragm spring clamping force and releasing force are simplified based on several hypothesis using A-L method and only one ideal curve is obtained. However, many uncertain factors will affect the performance. Particularly, the hysteresis phenomenon occurs during operation of diaphragm spring. When the pressure on the diaphragm spring is increased or decreased, the load characteristics are different, which is caused by internal friction in the spring material itself.

In order to further reveal the difference between the engaging and disengaging process, experiments on the clamping forces and the releasing forces are conducted and the results are shown in Figure 5.

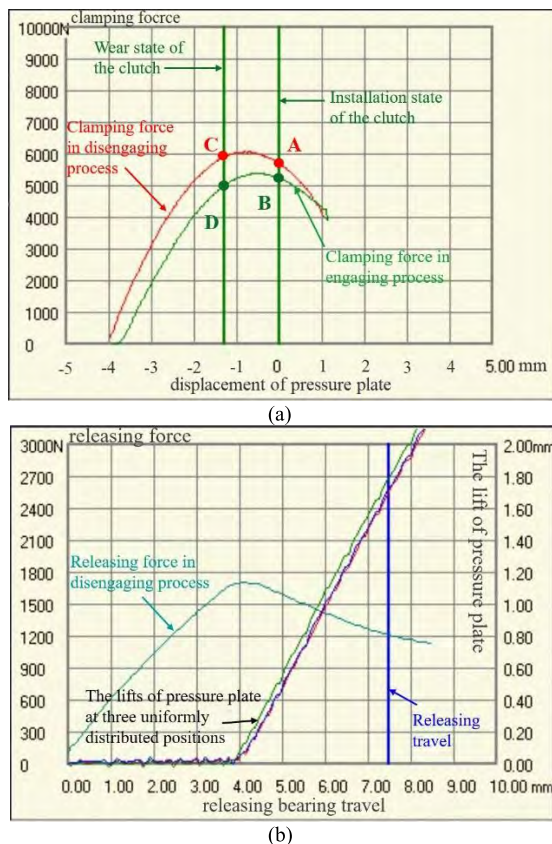


FIGURE 5. The test results of load and releasing characteristics of clutch cover assembly. (a) Characteristics of the clamping forces. (b) The releasing curves.

Figure 5 (a) shows the characteristics of the clamping force. There are two curves where the red upper curve is for the disengaging process and the lower green line is for the engaging process. It can be seen that the clamping force in the two process are different, shown as the differences between A and B, and between C and D, no matter the clutch is just installed or is in the wear state. This phenomenon is caused by the width of the pressure plate support, the co-axiality and the roundness of the support rings, the hysteresis of spring and so on. As a result, when calculate the transmitted torque using (12), F_{ppd} and F_{ppe} are adopted. Moreover, in order to make improve the robustness of the ability to transmit torque, the tolerance is controlled within $\pm 8\%$.

Figure 5 (b) shows the characteristics of the releasing forces. As the releasing forces in the disengaging process is larger than that during the engaging process, only the former is measured to calculate the pedal force. The peak of the cyan line is the maximum releasing force and the intersection point of the releasing force and the releasing travel is the force at the disengaging point. It should be noted that the zero travel of the pressure plate is caused by the deformation of the diaphragm spring resulting from the disengaging force.

To demonstrate the importance of separating the engaging and disengaging process and the influence on the clutch

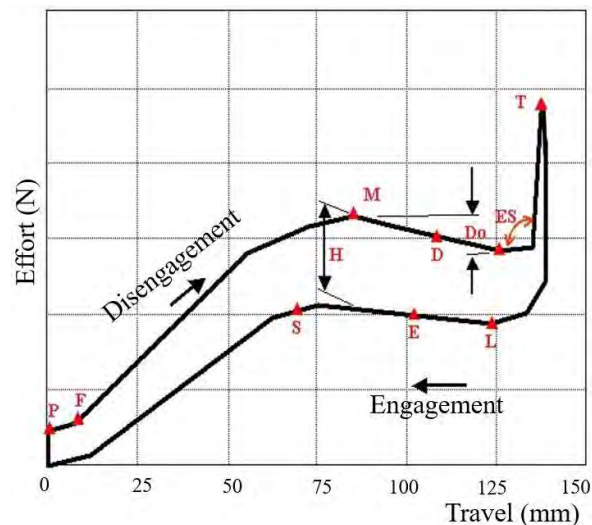


FIGURE 6. Clutch pedal manipulating curve.

TABLE 1. Clutch pedal manipulating curve parameter description.

Symbol	Description
T	Total Pedal Travel [mm]
D	Disengaged Travel D [mm]
M	Peak Force [N]*
L	Return Load [N]
D_0	Drop-Off Range from F_{max}
F	Freeplay [mm]
P	Pre-load Range [N]
E	Engaged Travel E [mm]
S	Stall Point S [mm]
H	Hysteresis [N]
ES	End Stop Shape [deg]

control, the transferred force and simulated pedal forces are shown in Figure 6 and the specific point descriptions are listed in Table 1.

It can be seen that the pedal forces in the disengaging process and the engaging process are different which matches the analysis of Figure 5. Moreover, the maximum disengaging pedal force is also in accordance with the releasing force of the clutch.

After the determination of the clutch specifications by the space constraints, the clamping force can be adjusted according to (12) where the clamping force, the releasing force and the pressure plate lift are related. The greater the lever ratio of the diaphragm spring is, the smaller the releasing force would be, as well as the pressure plate lift, which leads to the risk of incomplete disengagement. This feature requires a reasonable choice of the lever ratio and the adjustment of the relevant parameters of the releasing mechanisms. Adjusting the axial compressing characteristics of the cushion plate could also be an effective solution and the detailed analysis will be developed in the following sections

III. DETAILED COMPONENT MODELING AND INFLUENCE ANALYSIS

Considering the mechanical characteristics of clutch constituent components such as the diaphragm spring, the strap and the cushion plate have significant influence on the clutch engagement and disengagement processes which have been neglected by many literatures, the modeling and influence analysis of each part are conducted in this section.

A. DIAPHRAGM SPRING MODELING AND ANALYSIS

In the cover assembly, the clamping and releasing characteristics are mainly determined by the diaphragm spring [37] which is shown in Figure 7.

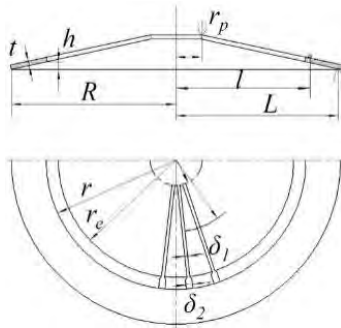


FIGURE 7. The diaphragm spring.

In Figure 7, t is thickness of the diaphragm spring, h is the truncated cone height of Belleville Spring part, R is the outer radius of diaphragm spring, r is the inner radius, L is the outer loading radius/contacting radius between the diaphragm spring and the pressure plate, l is the radius of support ring, r_p is the radius of the releasing bearing, r_e is the radius of the front releasing finger, δ_1 and δ_2 are the two widths between releasing fingers.

The relationship between the clamping force P_1 of the diaphragm spring and the outer edge deformation of the diaphragm spring is [38]

$$P_1 = \frac{\pi Et \lambda_1 \ln \frac{R}{r}}{6(1-\lambda^2)(L-l)^2} \left[\left(h - \lambda_1 \frac{R-r}{L-l} \right) \left(h - \frac{\lambda_2 R-r}{2(L-l)} \right) + t^2 \right] \quad (16)$$

where λ is the Poisson ratio, λ_1 is the outer edge deformation of diaphragm spring, E is the elastic modules.

The relationship between the releasing force P_2 of diaphragm spring and the outer edge deformation of the diaphragm spring is

$$P_2 = \frac{\pi Et \lambda_1 \ln \frac{R}{r}}{6(1-\lambda^2)(L-l)(l-r_p)} \left[\left(h - \lambda_1 \frac{R-r}{L-l} \right) \left(h - \frac{\lambda_2 R-r}{2(L-l)} \right) + t^2 \right] \quad (17)$$

The lever ratio of the diaphragm spring k is

$$k = \frac{l-r_p}{L-l} \quad (18)$$

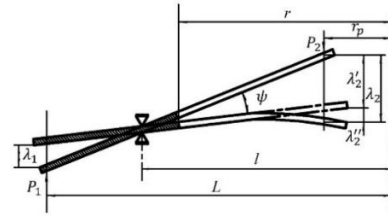


FIGURE 8. The small end deformation diagram of diaphragm spring.

The support point and clamping force point of diaphragm spring in the push-type clutch are shown in Figure 8. In the figure, ψ is the cone angle of the diaphragm spring.

The total deformation of inner edge λ_2 is made up of λ_2' and λ_2''

$$\lambda_2 = \lambda_2' + \lambda_2'' \quad (19)$$

The relationship between the axial deformation of the diaphragm spring λ_1 and the axial deformation of the diaphragm spring λ_2' at the contact point with the pressure plate is as follows:

$$\lambda_2' = \lambda_1 \frac{l-r_p}{L-l} \quad (20)$$

Substituting (20) into (17), the relation between the inner edge force P_2 and the inner displacement λ_2' is

$$P_2 = \frac{\pi Et \lambda_2' \ln \frac{R}{r}}{6(1-\lambda^2)(l-r_p)^2} \left[\left(h - \lambda_2' \frac{R-r}{l-r_p} \right) \left(h - \frac{\lambda_2' R-r}{2(l-r_p)} \right) + t^2 \right] \quad (21)$$

The bending deformation of inner edge of diaphragm spring λ_2'' under the force P_2 is

$$\lambda_2'' = \frac{6P_2 r_p^2}{\pi E h^3} \left\{ \frac{1}{\beta_1} \left[\frac{1}{2} \left(\frac{r_e^2}{r_p^2} - 1 \right) - 2 \left(\frac{r_e}{r_p} - 1 \right) + \ln \frac{r_e}{r_p} \right] + \frac{1}{\beta_2} \left[\frac{1}{2} \left(\frac{r^2}{r_p^2} - \frac{r_e^2}{r_p^2} \right) - 2 \left(\frac{r}{r_p} - \frac{r_e}{r_p} \right) + \ln \frac{r_e}{r_p} \right] \right\} \quad (22)$$

where β_1 and β_2 are the width coefficients,

$$\beta_1 = 1 - \frac{\delta_1 n}{\pi(r_p + r_e)}, \quad \beta_2 = 1 - \frac{\delta_2 n}{\pi(r_p + r)} \quad (23)$$

and n is the releasing finger number.

As the diaphragm spring has significant influence on the performance of the clutch, the manufacturing tolerance of the thickness of the material and the forming truncated angle cannot be neglected. According to the material standard, the tolerance of diaphragm spring thickness is ± 0.03 mm, and the average manufacturing angle tolerance of the diaphragm spring is $\pm 20'$. The detail specifications are given in Table 2.

The manufacturing tolerance would affect the clamping forces P_1 and the releasing force P_2 , and further affect the transmitted torque of the clutch.

TABLE 2. The main parameters of clutch and diaphragm spring.

Parameters	Value	Parameters	Value
t	2.52mm	Disc assembly thickness	6.7mm
R	94.535mm	Wear value	1.8mm
r	74.465mm	Releasing travel	7.5-8.5mm
L	93.5mm	Friction coefficient	0.42
l	75.5mm	Clamping force	4700N
ψ	12°	Cushion height	0.7mm
r_c	64.882mm	R_1	155mm
r_p	20mm	R_2	220mm
δ_1	3mm	δ_2	11mm

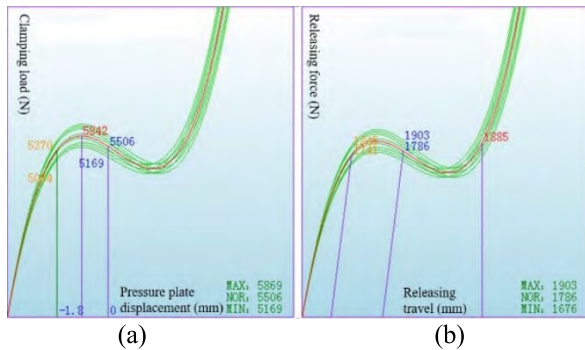


FIGURE 9. Load and releasing characteristics curve of diaphragm spring based on tolerance.

The simulated curves of the clamping force and releasing characteristics considering the manufacturing tolerance are shown in Figure 9.

Figure 9(a) shows the relations between clamping force and pressure plate displacement. The relations between releasing force and releasing travel are shown in Figure 9(b). There are nine clamping and releasing curves simulated including the nominal, the maximum and minimum material thicknesses and forming truncated angles. The red lines are the corresponding clamping force and releasing force curves of the nominated size and the green lines are for the sample sets within the tolerance. These curves could reveal the minimum friction torque, maximum releasing force and the corresponding ranges which could further help ensure the torque transmissibility and the manipulating comfort of the mass production to meet the functional requirements.

B. STRAP MODELING AND ANALYSIS

The hook clips in traditional clutches are removed in new developed clutches, instead, the straps, which have considerable influence on the dynamic performance and are rarely investigated in previous literature, will connect the clutch cover and the pressure plate and will also lift the pressure plate to achieve the release function.

The relationship between the strap force F_{st} and deformation of strap f_B is as follows [39]

$$F_{st} = k_a n_s \frac{E b_s h_s^3}{4 l_s^3} f_B \tag{24}$$

where k_a is the adjustment coefficient affected by the strap material, flatness and riveting force, n_s is the strap number, b_s is the strap width, h_s is the strap thickness, l_s is the distance between two holes of strap.

The clamping force F_{pp} and releasing force F_{cr} of cover assembly can be determined according to the cantilever beam analysis as follows

$$F_{pp} = P_1 - F_{st} \tag{25}$$

$$F_{cr} = F_{pp}/k = (P_1 - F_{st})/k \tag{26}$$

In order to reveal the effects caused by detailed analysis, the comparisons between the simplified model and the proposed model are shown in Figure 10 considering the load of diaphragm spring and the load of straps.

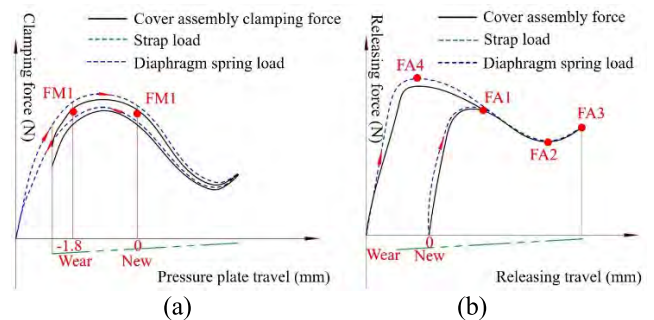


FIGURE 10. Comparison of (a) clamping force and (b) releasing force.

Figure 10 (a) shows the relations between the clamping force of cover assembly and the displacement of pressure plate. In most existing literature, the load of the diaphragm spring which is the blue dotted line was treated as the clamping and of the cover assembly, ignoring the bending force F_{st} from the deformation of the strap shown as the green line. The resultant bending force is opposite to the load of the diaphragm spring and would reduce the clamping force P_1 by 5% to 10%. This influence should be considered in the product design according to the specific situation. By considering the deformation of the strap, the resultant clamping force of the cover assembly is shown by the black solid line which is lower than the blue line. FM1 represents the required clamping force which is the mean of the clamping forces in the engaging and disengaging processes. It can be seen that with the wear of the clutch, FM1 moves to the left. Figure 10 (b) shows similar influence of the strap on the releasing force where FA1 is the maximum disengaging force for new clutch. FA2 is the minimum disengaging force. FA3 is the releasing at the maximum releasing travel and FA4 is the maximum disengaging force for wear clutch.

C. CUSHION PLATE MODELING AND ANALYSIS

The cushion plate will generate certain forces in axial direction during the engaging or disengaging process and will affect the performance of the clutch. As a result, the studies on the characteristics of the cushion plate could help investigate the dynamics of the clutch.

Because of the extremely irregular shape of cushion plate, it is complicated to define the relationship between the forces

and deformations. To solve this problem, the cushion plate can be properly simplified and divided into three parts, the part directly contacts the friction face, and the left and right parts beside the contacting part, as shown in Figure 11.

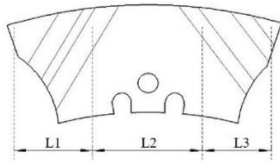


FIGURE 11. The simplified model of cushion spring.

Assume the left and right parts as cantilever plates, the relationship between the load and deformation can be derived. The flexural equation of the cantilever plate can be established by using the natural coordinates of the Euler-Bernoulli equation:

$$\frac{d\theta}{ds} = -\frac{M(s)}{D} \quad (27)$$

where D is the flexural rigidity of the model, and $D = D(s)$, s is the distance between the fixed end and the free end, θ is the angular displacement, and $M(s)$ is the bending moment.

$$D = \frac{Et_{cp}^3 b_{cp}}{12(1 - \lambda^2)} \quad (28)$$

where t_{cp} is the thickness of the cushion plate, b_{cp} is the width of the cushion plate.

When the large deflection is analyzed, the bending moment $M(s)$ of any section is.

$$M(s) = H_{cp} \cdot F_{cp} \quad (29)$$

where F_{cp} is the load from the cover assembly, H_{cp} is the horizontal distance from the free end to the s point and can be calculated by

$$H_{cp} = \int_0^s \cos \theta(\varepsilon) d\varepsilon \quad (30)$$

where ε is the length of the hypotenuse of the cushion plate.

Then the following equation can be obtained:

$$-D \frac{d^2\theta}{ds^2} = F_{cp} \cdot \cos \theta \quad (31)$$

The deflection of the free end and the horizontal displacement w are determined as

$$w = \int_0^q \sin \theta ds \quad (32)$$

$$u = \int_0^q (\cos \theta - 1) ds \quad (33)$$

where q is length of the cantilever plate.

$$w \approx \int_0^q \theta ds = q \sin \theta_m - \frac{F_{cp}}{2D} \left[\frac{1}{3} q^3 + q^2 \left(\sqrt{\frac{2D}{F_{cp}}} \sin \theta_m - q \right) + q \left(\sqrt{\frac{2D}{F_{cp}}} \sin \theta_m - q \right)^2 \right] \quad (34)$$

where θ_m is the angular displacement of the free end of the cantilever plate. The cushion characteristics of the cushion plate can be obtained by adjusting the deflection of the cushion plate w according to the settled load value.

To further investigate the effectiveness of the proposed method, the axial compression characteristics of the cushion plate are tested by using the cushion characteristics testing machine shown in Figure 12.



FIGURE 12. Testing machine of disc assembly.

The basic structural parameters and the material properties of cushion spring are shown in Table 3.

TABLE 3. The parameters of the cushion spring.

Width b_{cp} (mm)	Deflection w (mm)	Thickness t_{cp} (mm)	Poisson's ratio
23.4	0.7	0.8	0.282
Material	Density (t/ mm ³)	Elastic modulus (Mpa)	
65Mn	7.82e-9	1.97e5	

The testing machine mainly includes the loading mechanism, the clamping mechanism and the measuring mechanism. The disc assembly is loaded until the load reaches the specified clamping force, and the axial compression displacement and its corresponding axial compression load are recorded during this time, and the cushion characteristic curve is obtained. Figure 13 shows the comparisons between the simulated results (FE line) and the experimental measurement (EF line).

Table 4 shows the numerical error of the axial load of the cushion in the simulation analysis (FE) and the experimental measurement (EF).

TABLE 4. The error of the axial load of the simulation results and the experimental results.

Displacement (mm)	0.1	0.3	0.5	0.7
Load (N)/(FE)	272	972	1946	4769
Load (N)/(EF)	246	876	1786	4430
Error (%)	9.6	9.9	8.2	7.1

It can be seen that the trend of the simulated curve is very similar to the experiment result. In Table 4, the minimum load error between the simulation and the experiment is 7.1% and the maximum error is 9.9% which are within the

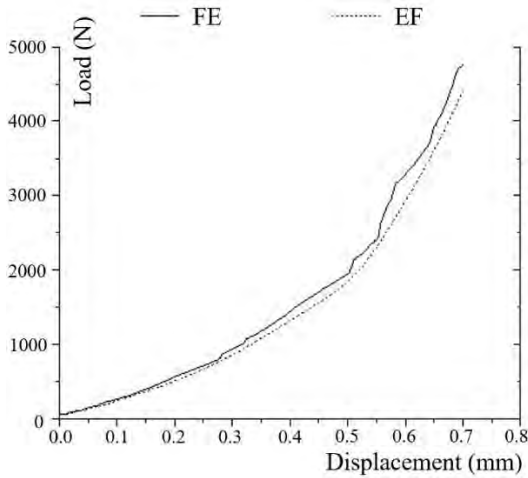


FIGURE 13. The axial compression comparisons of the cushion spring between simulation and experiment.

scope of the engineering application. There are many reasons for the error of simulation results, including the simplified simulation model and the uncertainty of the nonlinear contact parameters between the cushion plate and the friction face.

To further reveal the improvement of the detailed model of the cushion plate, the influence on the clutch engagement and disengagement processes is investigated. Assume the clutch engaging and disengaging velocities to be uniform, and the clamping force to be the corresponding deformation load of the cushion plate. When the cushion plate is fully compressed, the clamping force on the face is the clamping force of the cover assembly.

The releasing force of the clutch F_{rb} can be expressed as follows:

$$F_{rb} = F_{cr} - F(w) \tag{35}$$

where $F(w)$ is the transferred releasing force of the disc assembly. Together with (21) and (26), the following equation can be obtained:

$$F_{rb} = \frac{\pi Et\lambda'_2 \ln \frac{R}{r}}{6(1-\lambda^2)(l-r_p)^2} \left[\left(h - \lambda'_2 \frac{R-r}{l-r_p} \right) \left(h - \frac{\lambda'_2}{2} \frac{R-r}{l-r_p} \right) + t^2 \right] - F_{st/k} - F(w) \tag{36}$$

There is an approximate relationship between the displacement of the cushion plate w and the releasing travel λ_2 :

$$\lambda'_2 = w \frac{l-r_p}{L-l} \tag{37}$$

Combined with the releasing characteristics of the cover assembly and the characteristics of the cushion plate, the releasing characteristic comparisons are shown in Figure 14.

When the influence of the cushion plate is not considered, the releasing force will be the force of the cover assembly represented by the black solid line between C_1 and E in new installed state. However, this contradicts the facts. The reason

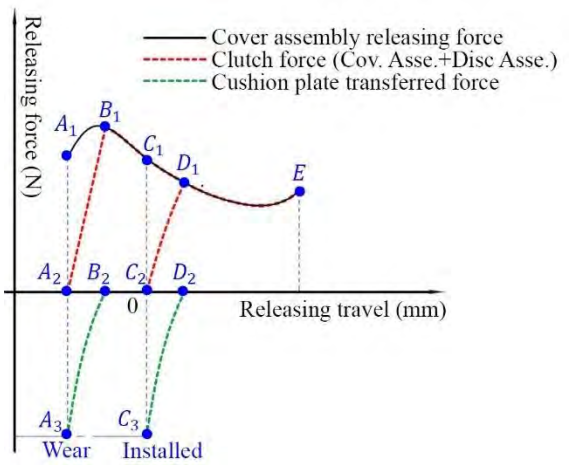


FIGURE 14. The disengagement characteristics of clutch.

is that the force of the cushion plate is opposite to the force of cover assembly and the values of them are set to be almost the same. The red line between C_2 and D_1 represents the actual force combining the effects of the cover assembly (the black line between C_1 and E) and the cushion plate (the green line between C_3 and D_2). It can be seen that due to the cushion plate, C_1 is moved to C_2 . For D_1 , as the deformation of the cushion plate at D_2 is 0, it will not be affected. As the cushion characteristic would not change much during the lifespan shown as A_3 and B_2 , when the clutch is in wear state (black line between A_1 and C_1), the actual clutch force would move to the left as shown by the red line between A_2 and B_1 .

IV. EXPERIMENTS AND ANALYSIS OF THE CLUTCH ENGAGEMENT AND DISENGAGEMENT CHARACTERISTICS

In order to evaluate the performance of the proposed detailed mathematical model and the effectiveness of dividing the clutch engaging process into four stages, experiments have been carried out. The first experiment is to test the transmitted torque which can be used to evaluate the accuracy of the proposed model. The second experiment is about the pedal force control during gear shifting to demonstrate the necessity to treat the disengaging process separately.

A. TRANSMITTED TORQUE EVALUATION

In the experiment which is shown in Figure 15, a new cover assembly and disc assembly are fixed in the testing bench of clutch characteristics which can measure rotating torque and angular speed.

The maximum torque of the engine is 225 Nm, the engaged speed is 800 r/min, the moment of inertia is 5.25 kg·m², the clutch cycle time is 30 s. In accordance with the specified conditions, the clutch should be engaged and synchronized, then disengaged and braked to stop, indicating that a cycle is finished. The cycle is repeated 60 times. The curves of

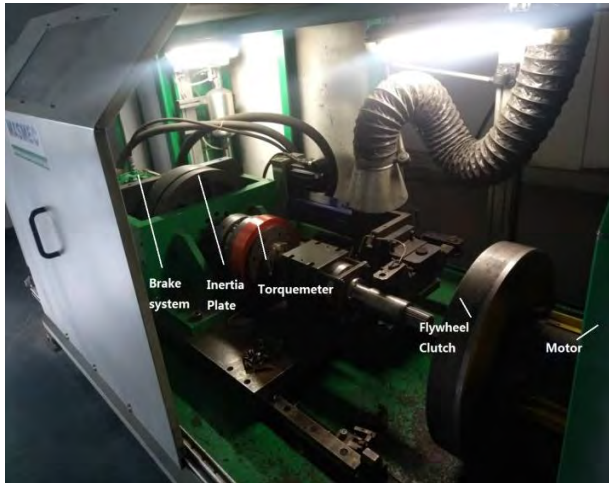


FIGURE 15. Testing bench of clutch characteristics.

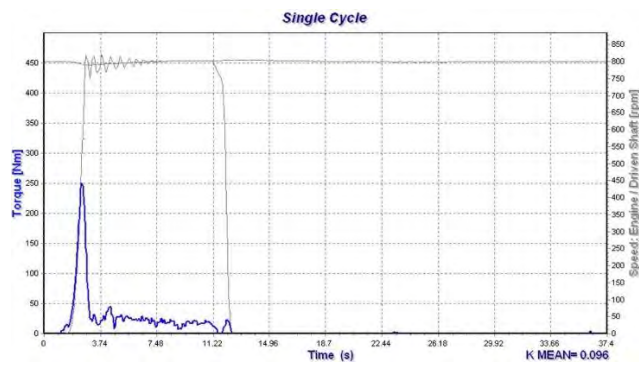


FIGURE 16. The testing results of clutch characteristics.

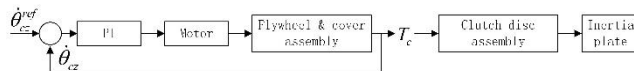


FIGURE 17. Closed-loop PI controller.

velocity and torque with time are recorded. The result of a selected cycle is shown in Figure 16.

The engaged time is 1.55 S, and the disc assembly of clutch is synchronized with the cover assembly. The maximum torque is 249.78 Nm, while the clutch friction coefficient is 0.42. The outside diameter of friction facing is 220 mm, inner diameter is 155 mm, the force is concluded to 3140.4 N according to (13). The displacement of the cushion plate is about 0.62mm according to the test curve in Figure 13. As a comparison, the simulation results of the proposed method in shown in Figure 17. In the simulation model built in Simulink, four degrees of freedom (DoFs) are used to describe the rotating motions of the motor, flywheel, clutch cover and inertia plate in the testing bench. This model integrates the clutch torque model and the characteristics of the strap, diaphragm spring and cushion plate. When the pressure plate starts to contact the friction face and compress the cushion spring, the clutch torque is transmitted from the driving

source (motor) to the driven side (clutch disc assembly and inertia plate). As the clutch engagement process finishes, the flywheel and clutch cover assembly are fixed together under the clamping force generated by the diaphragm spring, thus they rotate at the same speed.

In addition to the detailed model, control scheme is another important aspect. Different from the complex control method in literature [40], [41], a simple PI controller shown in Figure 17 is applied in this paper to keep the flywheel rotating at a constant speed during engagement and disengagement. The motor is under the speed mode, thus the motor can actively adjust the output torque according to the external load and the difference between the current rotating speed and desired speed. This speed difference can be obtained by the speed feedback. Consequently, the motor can adjust the speed to the desired level. It should be noted that the motor can adjust its output torque actively based on the flywheel rotating speed and the load acting on it, i.e. the torque transmitted by the clutch, T_c .

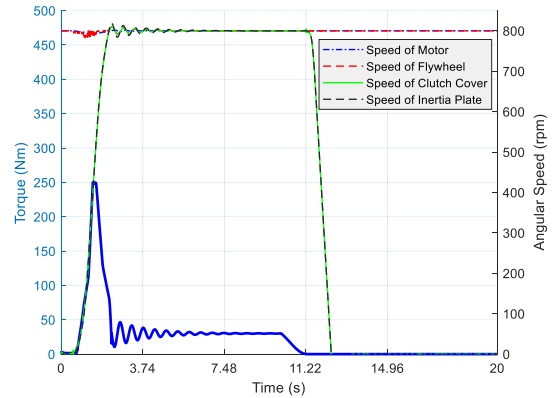


FIGURE 18. The simulation results of clutch engagement.

When the clutch finishes the disengaging process, a breaking torque acts on the inertia plate, thus its rotating speed decreases significantly and finally arrives zero, indicating that a cycle is finished. Figure 18 also displays the simulated torque response transmitted by the friction clutch during engagement, and the torque peak is about 250 Nm. After engagement, the motor reduces the output torque to keep the inertia plate rotating at a constant speed (800 rpm), resulting in the significant decrease of the clutch torque (less than 50 Nm). Then, the torque reduces to zero before the disengagement phase (around 11.22s). Then the flywheel and clutch cover assembly are separated completely. By comparing Figure 16 and Figure 17, the simulation results of the newly established detailed model are consistent with the experimental results, which validates the effectiveness of the proposed detailed mathematical model. A conclusion can be drawn that the important components (diaphragm spring, strap, cushion spring, etc.) have considerable influences on the clutch engagement or disengagement characteristics. Therefore, in order to improve the analysis accuracy, these influences should be taken into consideration.



FIGURE 19. The testing bench of clutch pedal control.

B. CLUTCH PEDAL FORCE EVALUATION

Clutch manipulate system is to realize the clutch engagement and disengagement. And the factors affecting clutch manipulating comfort mainly includes the clutch pedal position, pedal travel and the pedal force. The related researches are considered in terms of the perspective of ergonomics. The tester as shown in Figure 19 is fixed on the car, including displacement sensor and force sensor. The measure system transmits the data to the industrial personal computer which processes relevant data through special software. In the experiment, the clutch pedal is step down and slowly released. In this process, the specified position is selected, and the corresponding pedal travel and pedal force are measured. The content of pedal travel measurement includes clutch engagement travel, clutch separation point travel, pedal total travel, etc. The corresponding position is selected for pedal force measurement, and the corresponding pedal travel and pedal force are measured respectively. Then the curve can be acquired as shown in Figure 20 where the annotations are shown in Table 1.

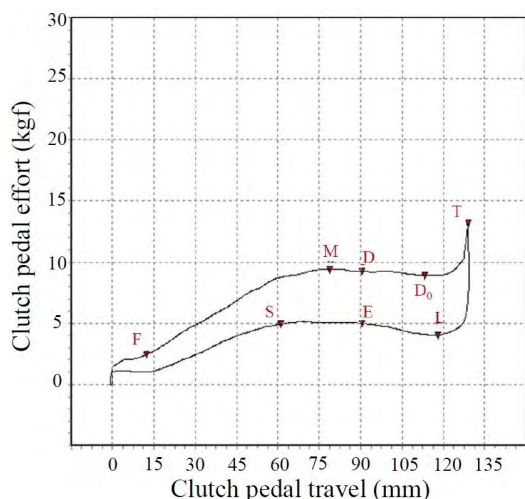


FIGURE 20. The testing result of clutch control.

The test results show that the design requirements can be met from the perspective of ergonomics shown in Figure 6. Through the analysis of the previous relevant mechanical model and the determination of the evaluation method of manipulate comfort, the manipulate comfort of the manual

transmission can be improved and a basis for the control of the automatic transmission can be provided. It can be summarized that the proposed detailed analysis could reveal the influences of the manufacturing tolerance on the characteristics of torque transmissibility and how the corresponding components actually affect the transmitted torque, which makes it possible to accurately decide the clutch releasing force and travel, meet the requirements of smooth torque transmit and cut off, and determine the reasonable safety coefficient. Moreover, optimal control solutions of manual transmission for handling comfort could be found by investigating the clutch pedal manipulating curve, and for automatic transmission like AMT which also adopts the clutch system, the revealed clutch characteristics such as the actual torque, force and deflection curves of each components could be used to improve the control profile to reduce the vehicle jerk caused by the clutch engagement and disengagement.

V. CONCLUSION

The paper focuses on the analysis and evaluation of engagement/disengagement characteristics of the dry clutch. First of all, considering the differences of sliding factors in the clutch engagement/disengagement process, the four states dynamics model and the mechanical equation of clutch processes are established. Then, on this basis, the clamping force and releasing force characteristics of the clutch are analyzed, the dynamic formula of dry clutch in four states are derived according to the uniform pressure method, and the system solution of dry clutch torque transmissibility and pedal operation comfort is put forward. Moreover, in order to improve the accuracy of the analysis, influences of key parts such as diaphragm spring, strap and cushion plate on clutch engagement/disengagement characteristics are investigated according to the FE analysis based on the modeling and the corresponding mechanical properties. The correction formula of A-L method is used based on the key size tolerance of diaphragm spring and considered wear properties in the life cycle. The mechanical model and formula derivation of cushion plate as the key part of the disc assembly have been carried out, and the simulation and experimental verification have been performed. At last, the test method of the clutch torque and the pedal travel and the pedal force was put forward to evaluate the engagement and disengagement characteristics of the dry clutch. The clutch torque test on the bench and the pedal travel and force test on the vehicle are carried on. This study can help improve the torque transmission stability and manipulate comfort of manual transmission and provide theoretical basis for the control of automatic transmission.

The contributions of this paper mainly include three aspects: 1) The hysteresis characteristics of diaphragm spring is considered in this study, and the influence of manufacturing tolerance of diaphragm spring on the clamping forces and the releasing force are quantitatively studied. To the best of our knowledge, the tolerance influence is ignored in the previous literature. 2) The nonlinear load characteristics of cushion spring obtained from simulation results and

experiment measurement are compared to validate the effectiveness of cushion mathematical model. 3) A detailed model is built to study the impacts of subsystems on the clutch engaging performance, which includes the clutch torque model and the characteristics of diaphragm spring, cushion spring and straps. Hence, this detailed model has higher accuracy in estimating the dynamics behavior of a clutch engagement than the traditionally simplified clutch model only includes the torque model.

REFERENCES

- [1] M. Awadallah, P. Tawadros, P. Walker, and N. Zhang, "Dynamic modelling and simulation of a manual transmission based mild hybrid vehicle," *Mech. Mach. Theory*, vol. 112, pp. 218–239, Jun. 2017.
- [2] S. Lin, S. Chang, and B. Li, "Improving the gearshifts events in automated manual transmission by using an electromagnetic actuator," *Proc. Inst. Mech. Eng. C, J. Mech. Eng. Sci.*, vol. 229, no. 9, pp. 1548–1561, Mar. 2015.
- [3] W. Cao et al., "Speed synchronization control for integrated automotive motor-transmission powertrains over can through a co-design methodology," *IEEE Access*, vol. 6, pp. 14106–14117, 2018.
- [4] J. Freitag, F. Gerhardt, M. Hausner, and C. Wittmann, "The clutch system of the future," in *Proc. 9th Schaeffler Symp.*, 2010, pp. 1–10.
- [5] J. Liang, H. Yang, J. Wu, N. Zhang, and P. D. Walker, "Power-on shifting in dual input clutchless power-shifting transmission for electric vehicles," *Mech. Mach. Theory*, vol. 121, pp. 487–501, Mar. 2018.
- [6] C.-M. Ning, Z.-Q. Chao, H.-Y. Li, and S.-S. Han, "Control performance and energy-saving potential analysis of a hydraulic hybrid luffing system for a bergepanzer," *IEEE Access*, vol. 6, pp. 34555–34566, 2018.
- [7] O. H. Dagci, H. Peng, and J. W. Grizzle, "Hybrid electric powertrain design methodology with planetary gear sets for performance and fuel economy," *IEEE Access*, vol. 6, pp. 9585–9602, 2018.
- [8] A. Myklebust and L. Eriksson, "Modeling, observability, and estimation of thermal effects and aging on transmitted torque in a heavy duty truck with a dry clutch," *IEEE/ASME Trans. Mechatronics*, vol. 20, no. 1, pp. 61–72, Feb. 2015.
- [9] M. Pisaturo, C. D'Auria, and A. Senatore, "Friction coefficient influence on the engagement uncertainty in dry-clutch AMT," in *Proc. Amer. Control Conf. (ACC)*, Jul. 2016, pp. 7561–7566.
- [10] A. D. Gatta, L. Iannelli, M. Pisaturo, A. Senatore, and F. Vasca, "A survey on modeling and engagement control for automotive dry clutch," *Mechatronics*, vol. 55, pp. 63–75, Nov. 2018.
- [11] M. Pisaturo, M. Cirrincione, and A. Senatore, "Multiple constrained MPC design for automotive dry clutch engagement," *IEEE/ASME Trans. Mechatronics*, vol. 20, no. 1, pp. 469–480, Feb. 2015.
- [12] H. Chen and B. Gao, "Clutch disengagement timing control of AMT gear shift," in *Nonlinear Estimation and Control of Automotive Drivetrains*. Berlin, Germany: Springer, 2014, pp. 147–156.
- [13] L. Li, X. Wang, X. Qi, X. Li, D. Cao, and Z. Zhu, "Automatic clutch control based on estimation of resistance torque for AMT," *IEEE/ASME Trans. Mechatronics*, vol. 21, no. 6, pp. 2682–2693, Dec. 2016.
- [14] Z. Zhao, L. He, Y. Yang, C. Wu, X. Li, and J. K. Hedrick, "Estimation of torque transmitted by clutch during shifting process for dry dual clutch transmission," *Mech. Syst. Signal Process.*, vol. 75, pp. 413–433, Jun. 2016.
- [15] J. Liang, H. Yang, J. Wu, N. Zhang, and P. D. Walker, "Shifting and power sharing control of a novel dual input clutchless transmission for electric vehicles," *Mech. Syst. Signal Process.*, vol. 104, pp. 725–743, May 2018.
- [16] J. Liang, P. D. Walker, J. Ruan, H. Yang, J. Wu, and N. Zhang, "Gearshift and brake distribution control for regenerative braking in electric vehicles with dual clutch transmission," *Mech. Mach. Theory*, vol. 133, pp. 1–22, Mar. 2019.
- [17] H. Wu, P. Walker, J. Wu, J. Liang, J. Ruan, and N. Zhang, "Energy management and shifting stability control for a novel dual input clutchless transmission system," *Mech. Mach. Theory*, vol. 135, pp. 298–321, May 2019.
- [18] J. Deur, V. Ivanović, F. Assadian, M. Kuang, E. H. Tseng, and D. Hrovat, "Bond graph modeling of automotive transmissions and drivelines," *IFAC Proc. Vols.*, vol. 45, no. 2, pp. 427–432, 2012.
- [19] B. Mashadi and D. Crolla, *Vehicle Powertrain Systems*. Hoboken, NJ, USA: Wiley, 2012.
- [20] P. D. Walker, N. Zhang, and R. Tamba, "Control of gear shifts in dual clutch transmission powertrains," *Mech. Syst. Signal Process.*, vol. 25, no. 6, pp. 1923–1936, 2011.
- [21] M. Pisaturo and A. Senatore, "Simulation of engagement control in automotive dry-clutch and temperature field analysis through finite element model," *Appl. Therm. Eng.*, vol. 93, pp. 958–966, Jan. 2016.
- [22] K. Van Berkel, T. Hofman, A. Serrarens, and M. Steinbuch, "Fast and smooth clutch engagement control for dual-clutch transmissions," *Control Eng. Pract.*, vol. 22, pp. 57–68, Jan. 2014.
- [23] F. Vasca, L. Iannelli, A. Senatore, and G. Reale, "Torque transmissibility assessment for automotive dry-clutch engagement," *IEEE/ASME Trans. Mechatronics*, vol. 16, no. 3, pp. 564–573, Jun. 2011.
- [24] X. Zhou, P. Walker, N. Zhang, B. Zhu, and J. Ruan, "Numerical and experimental investigation of drag torque in a two-speed dual clutch transmission," *Mech. Mach. Theory*, vol. 79, pp. 46–63, Sep. 2014.
- [25] J. Li, Y. Wang, and Y. Wang, "Optimal control for jitter suppression of clutch engagement in upshift process of electric vehicles," *Adv. Mech. Eng.*, vol. 8, no. 12, 2016, Art. no. 1687814016674847.
- [26] Y. He, D. Sun, M. Zhao, and S. Cheng, "Cooperative driving and lane changing modeling for connected vehicles in the vicinity of traffic signals: A cyber-physical perspective," *IEEE Access*, vol. 6, pp. 13891–13897, 2018.
- [27] S.-D. Lee and S.-L. Kim, "Characterization and development of the ideal pedal force, pedal travel, and response time in the brake system for the translation of the voice of the customer to engineering specifications," *Proc. Inst. Mech. Eng. D, J. Automobile Eng.*, vol. 224, no. 11, pp. 1433–1450, 2010.
- [28] R. Pannetier and X. Wang, "A comparison of clutching movements of freely adjusted and imposed pedal configurations for identifying discomfort assessment criteria," *Appl. Ergonom.*, vol. 45, no. 4, pp. 1010–1018, 2014.
- [29] X. Wang, B. Le Breton-Gadegbeku, and L. Bouzon, "Biomechanical evaluation of the comfort of automobile clutch pedal operation," *Int. J. Ind. Ergon.*, vol. 34, no. 3, pp. 209–221, 2004.
- [30] H. Zhang and J. Wang, "Vehicle lateral dynamics control through AFS/DYC and robust gain-scheduling approach," *IEEE Trans. Veh. Technol.*, vol. 65, no. 1, pp. 489–494, Jan. 2016.
- [31] J. Zhou, C. Wang, and J. Zhu, "Multi-objective optimization of a spring diaphragm clutch on an automobile based on the non-dominated sorting genetic algorithm (NSGA-II)," *Math. Comput. Appl.*, vol. 21, no. 4, p. 47, 2016.
- [32] L. Gerez and M. Liarokapis, "A compact ratchet clutch mechanism for fine tendon termination and adjustment," in *Proc. IEEE/ASME Int. Conf. Adv. Intell. Mechatronics (AIM)*, Jul. 2018, pp. 1390–1395.
- [33] P. J. Dolcini, C. Canudas-de-Wit, and H. Béchard, *Dry Clutch Control for Automotive Applications*. Berlin, Germany: Springer, 2010.
- [34] A. Myklebust, "Modeling and estimation for dry clutch control," Linköping Univ. Electron. Press, Seattle, WA, USA, Tech. Rep., 2013.
- [35] F. Vasca, L. Iannelli, A. Senatore, and M. T. Scafati, "Modeling torque transmissibility for automotive dry clutch engagement," in *Proc. Amer. Control Conf.*, Jun. 2008, pp. 306–311.
- [36] L. Weixin, "Automobile design," Tsinghua Univ. Press, Beijing, China, Tech. Rep., 2001.
- [37] L. Shi-Yu, "Diaphragm spring and Belleville spring clutches design and manufacturing," Southeast Univ. Press, Nanjing, China, Tech. Rep., 1995.
- [38] W. Yong-Hai, "Multi-objective optimization design of vehicle clutch diaphragm spring," in *Proc. 2nd Int. Conf. Intell. Comput. Technol. Automat.*, vol. 3, Oct. 2009, pp. 194–197.
- [39] D. Gross, W. Ehlers, P. Wriggers, J. Schröder, and R. Müller, *Mechanics of Materials—Formulas and Problems* (Engineering Mechanics), vol. 2. Berlin, Germany: Springer, 2017.
- [40] L. Li, X. Wang, X. Hu, Z. Chen, J. Song, and F. Muhammad, "A modified predictive functional control with sliding mode observer for automated dry clutch control of vehicle," *J. Dyn. Syst. Meas. Control*, vol. 138, no. 6, 2016, Art. no. 61005.
- [41] X. Wang, L. Li, K. He, and C. Liu, "Dual-loop self-learning fuzzy control for AMT gear engagement: Design and experiment," *IEEE Trans. Fuzzy Syst.*, vol. 26, no. 4, pp. 1813–1822, Aug. 2018.



ZHENG FENG YAN received the B.Sc. degree in mechanical engineering from the University of Chongqing, in 1991, the M.Sc. degree in industrial engineering from the Huazhong University of Science and Technology, in 2003, and the Ph.D. degrees in mechanical manufacturing and automation from the Wuhan University of Technology, in 2009. Since 2011, he has been a Full Professor with the Department of Vehicle Engineering, Hefei University of Technology. He has authored over

30 peer-review indexed journals, international conferences, and book chapters. He has also been participating in over 10 research projects funded by the regional and national government and companies. His current research interests include automotive components design and manufacturing, advanced manufacturing technology, and product development and design.



FUWU YAN is currently the Head of the School of Automotive Engineering, Wuhan University of Technology, where he is also a Full Professor of automotive engineering. His research interests include engine emission control technology, engine performance, and electronic control technology, electrification of vehicles, and powertrain design.

Dr. Yan has received several awards and honors, including the Vice President of the Hubei Institute of Internal Combustion Engine, the Director of Motorcycle Branch of China Association of Automobile Engineering, and the Executive Director of the Hubei Automobile Engineering Association.



JIEJUNYI LIANG received the B.S. degree in mechanical design, manufacturing and automation from the Huazhong University of Science and Technology, Wuhan, China, in 2012, the M.S. degree in electromechanical engineering from the University of Macau, Macau, China, in 2015, and the Ph.D. degree in mechanical engineering from the School of Mechanical and Mechatronic Engineering, University of Technology Sydney, in 2018. He is currently a Research Fellow with

the School of Automotive Engineering, Wuhan University of Technology, China.



YALIN DUAN received the M.Sc. degree in mechanical engineering from the Hefei University of Technology, in 2018. He has been with the Development Department of JATCO (Guangzhou) Automatic Transmission Ltd. His current work mainly focuses on automatic transmission experiment and product development. His research interests include automotive transmission systems, vehicle experiment, and finite element analysis.

• • •